International Journal of Microwave and Wireless Technologies

cambridge.org/mrf

Cylindrical conformation and miniaturization of cavity-backed magnetoelectric antenna with an outer Γ-shaped probe

Alexandre Causse[1,2], Loïc Bernard[1,2], Sylvain Collardey[2] and Ala Sharaiha[2]

[1]STC department, French-German Research Institute of Saint-Louis, Saint-Louis, France and [2]IETR, UMR CNRS 6164, University of Rennes 1, Rennes, France

Research Paper

Cite this article: Causse A, Bernard L, Collardey S, Sharaiha A (2024) Cylindrical conformation and miniaturization of cavity-backed magnetoelectric antenna with an outer Γ-shaped probe. *International Journal of Microwave and Wireless Technologies* **16**(2), 348–356. https://doi.org/10.1017/S1759078723001265

Received: 24 February 2023
Revised: 20 October 2023
Accepted: 20 October 2023

Keywords:
cavity; conformal antenna; GNSS; magnetoelectric antenna; wideband

Corresponding author: Loïc Bernard;
Email: loic.bernard@isl.eu

Abstract

In this article, the cylindrical conformation of a linearly polarized cavity-backed magnetoelectric (ME) antenna is studied. Starting from a planar ME antenna presenting a wide bandwidth due to a specific design of its feeding probe, the impact of conformation is shown; the coupling between the ME dipole and the cavity walls is demonstrated to be the key element to keep a wideband behavior. Conformal antennas offering the same impedance bandwidth as the planar antenna are presented operating at Global Navigation Satellite System frequencies (1.164–1.61 GHz). As a result of the conformation, the antenna size has to be reduced to maintain the coupling and a wideband behavior. A prototype conformed to a 44-mm radius cylinder was built using low-cost additive manufacturing. External dimensions of 62 × 62 × 35 mm^3 ($0.285 \times 0.285 \times 0.16\lambda_0{}^3$, where λ_0 is the wavelength at 1.38 GHz) were obtained, showing a ground plane area reduction of 46% compared to the planar antenna with the same materials. The conformal antenna also exhibits very steady radiation properties with a gain of around 4.5 dBi and a very similar and stable 3 dB beamwidth around 113° in E- and H-planes. A relatively good agreement is found between measurements and simulation.

Introduction

The Global Navigation Satellite Systems (GNSS) are nowadays an accurate and convenient solution for the navigation of a diversity of vehicles, from heavy to light ones and from huge to small ones, evolving in the sky [1], on the ground [2], or even under water [3]. Integration of a multiband antenna on these carriers may be a hard task, especially when the geometry is complex and, above all, when the available space is limited. Planar antennas are well adapted to large structures, whereas conformal ones are required for small cylinder platforms [4].

Cavity-backed antennas are of interest for integration purposes, as they enable the radiating element to be isolated from its direct surrounding environment, but the cavity can create limitations in terms of impedance bandwidth, for example. Conformation of the antenna to a specific shape minimizes aerodynamic drag by being mounted on or embedded in the curved surface and provides superior radio frequency (RF) performance.

A ME antenna [5] is interesting for GNSS applications as it has very uniform radiation properties versus frequency close to a Huygens source and a relatively large impedance bandwidth. Moreover, for some specific case scenarios such as medium- or high-altitude Unmanned Aerial Vehicles (UAVs), where the environment can be considered as multipath-free, linearly polarized antennas can be used for GNSS applications although satellite signals are circularly polarized at the cost of 3 dB power loss in the link budget.

The ME dipole, introduced in 2006 [5], aims to combine an electric and a magnetic dipole to obtain both an impedance wideband behavior, due to the combination of two close resonances, and very stable radiation properties. However, the main drawback was its large electrical size, as the structure needs a large ground plane to work properly.

Evolutions were proposed to decrease the profile of the radiating element by meandering or tilting the magnetic dipole [6–8] or adding metamaterial to reduce the overall size [9]. In particular, many different structures with diverse polarizations designed for base station antennas are presented in the study by Luk and Wu [8]. Miniaturization was also achieved by creating multiple close resonances with the addition of parasitic elements [10]. This leads to antennas combining a ME radiating element with other types of antennas. In the study by Tao et al. [11], the addition of parasitic element over the ME source creates a Yagi–Uda configuration and an impedance dual-band behavior. Modifications on the exciting probe were also investigated with, for example, a double Γ-probe [12], stair-shaped probe [13], or fork shape probe [14], which enables dual-band behavior and an antenna matched to 50 Ω for all GNSS bands and telemetry L and S bands (1.16–1.61 GHz and 2.2–2.4 GHz).

These modifications change the radiating properties of the classical ME structure.

Cavity-backed configurations of the ME were also investigated, often with large dimensions for the cavity, which can be with different heights to increase the bandwidth of the antenna [15] or conformal with circular array configuration [16]. Cavity-backed antenna in a smaller cavity is proposed in [17] by combining a specific placement of the probe outside the magnetic dipole and substrate to reduce the electrical size of the elements. For this last structure, three resonances are excited in the band of interest (instead of two for conventional ME antennas and cavity-backed ME antennas), presenting a wider bandwidth than conventional ME antennas of the same dimensions.

Cylindrically conformed patch antennas are also used in linear polarization for positioning L-band applications in single- and dual-band configurations [18, 19]. These antennas exhibit a low profile but cannot be used in GNSS multiple constellation application cases because their bandwidth remains very narrow. Besides, considering a printed antenna on a cylinder with a radius smaller than half of a wavelength, higher-order modes appear and become not anymore negligible, shifting the patch resonance frequency and affecting radiation characteristics [1, 20].

Whereas the concept of ME antenna and its design are well known in planar configuration, to the authors' knowledge, cylindrical ME antenna was not reported before the recent publication of Feng et al. [16]. In this last article, a conformal ME dipole is presented within a cylinder radius corresponding to $0.49\lambda_0$, whereas the ground plane is of $0.71\lambda \times 0.70\lambda$ at the central frequency.

In this article, we show the impact of the conformation on small cylinders (with radius from 0.46λ to 0.18λ) of a wideband linearly polarized cavity-backed ME antenna with a Γ-shape probe located outside of the magnetic dipole [17] and on the performance and the importance of the size of the cavity and of the walls. The coupling between the ME dipole and the cavity walls is demonstrated to be the key phenomenon to keep three resonances with an impedance close to 50 Ω, and finally, the cavity size reduction has proven to be an effective solution to maintain this coupling over a wide band. Well-integrated antennas presenting a cylindrical shape, compact and with good performances are obtained. The conformation enables the proposed antennas to be flush mounted on cylindrical carriers having small radius compared to the wavelength. In section "Planar antenna," the planar reference antenna dimensions and performances are presented. In section "Study of conformation," a study of the impact of conformation is proposed. First, the influence of cavity wall height on the input impedance of a planar antenna is shown, and then the conformal case is studied. It is shown that the evolutions of behavior due to the conformation on small cylinders (from 0.46 λ to 0.18 λ) lead to a miniaturization of the ground plane of the antenna while keeping close impedance bandwidth. In section "Optimized antenna and measurement results," an optimized conformal antenna (radius 44 mm) is presented, and simulation results are compared to measurements. Finally, a conclusion of this work is proposed in section "Conclusion." This article is an extension of the work [21] already proposed by the same authors.

Planar antenna

The reference planar antenna is a ME dipole antenna with a Γ-shaped probe placed outside of the magnetic dipole, as can be seen in Fig. 1. This specific location enables the enhancement of the antenna bandwidth by inducing a third well-controlled resonance in the band of interest of the antenna, as described in the study by Feng et al. [16], thus enhancing the bandwidth in comparison to conventional ME antennas of the same dimensions. All dimensions are shown in Table 1. The cavity is fulfilled by a dielectric material fabricated using 3D printer filament Preperm ABS300 ($\varepsilon_r = 3$ and $\tan\delta = 4.6 \times 10^{-3}$). The electric dipole resonates in $\lambda_g/2$ (where λ_g is the guided wavelength in the substrate) at 1.12 GHz, as the excitation probe placement combined with the cavity makes the resonant length equal to $(2 \times L_{dip} + W_{dip}/2)$ and reduces the length L_{dip} of the electric dipole compared to that obtained in the study by Luk and Wu [5]. The magnetic dipole resonates in $\lambda_g/4$ at 1.45 GHz, and the probe resonates in $\lambda_g/4$ at 1.7 GHz. The input impedance and the S_{11} parameter magnitude are shown in Fig. 2. The simulations are performed using Ansys HFSS [22]. The E-plane is the YoZ one according to the coordinate system shown in Fig. 1. The cavity walls are made of copper, as are the radiating elements, and they present a height H_E on XoZ plane and H_H in YoZ plane.

The reference antenna exhibits an impedance bandwidth ($|S_{11}| < -10$ dB) of 39.0% from 1.13 to 1.67 GHz and external

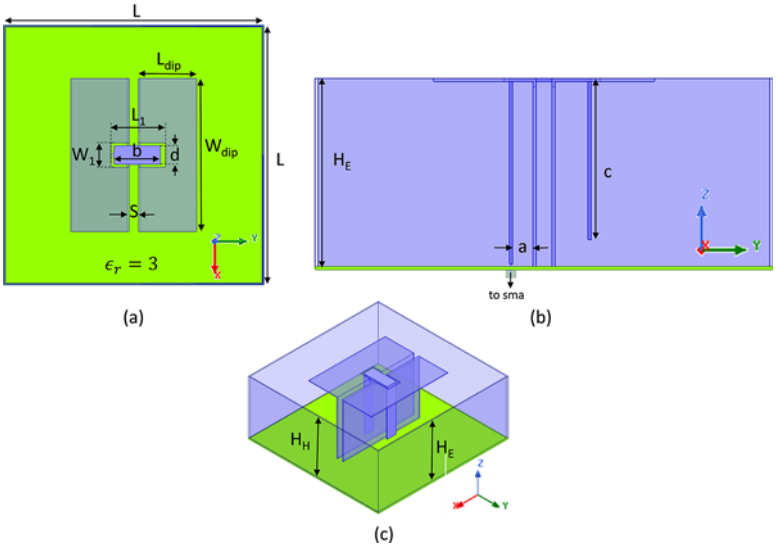

Figure 1. Top view (a), side view (b), and 3-D view (c) of the reference magnetoelectric dipole antenna.

https://doi.org/10.1017/S1759078723001265 Published online by Cambridge University Press

Table 1. Dimensions of the reference antenna

Parameter	Value (mm)	Parameter	Value (mm)
L	85	W_1	8
H_E	35	a	4.3
H_H	35	b	14
L_{dip}	19	c	28.7
W_{dip}	50	d	6
S	3	t	0.6
L_1	16	–	–

dimensions of 85 × 85 × 35 mm^3 (0.39 × 0.39 × 0.16λ_0^3 at the center frequency of 1.38 GHz). The broadside gain of the reference antenna and the 3-dB beamwidth versus frequency are shown in Fig. 3.

The obtained results are in adequation with the behavior of classical ME antenna with a very steady realized gain of around 5.2 dBi and 3-dB beamwidth over 90° with close values in E- and H-planes of the antenna (respectively, XoZ and YoZ planes). This planar antenna will be compared with conformal evolutions in terms of matching and radiation properties.

Study of conformation

This study aims to characterize the impact of cylindrical conformation on the input impedance and radiation properties of cavity-backed ME antenna. Starting from the optimized planar antenna presented in section "Planar antenna," first, the impact of the modification of wall height is investigated based on the study by Feng et al. [16]. This will be helpful to apprehend in a second time the case of a conformal antenna for which the cavity height is lower along the longitudinal axis; the approach is applied to fully conformal structures in the second part of this section.

Planar case

The variation of cavity height for a planar antenna with fixed ground plane dimensions was proposed by Causse et al. [20] (for a similar antenna filled with polypropylene and of dimensions 75 × 75 × 40 mm^3). From this study, it can be concluded that the variation of height for the cavity walls parallel to the exciting probe

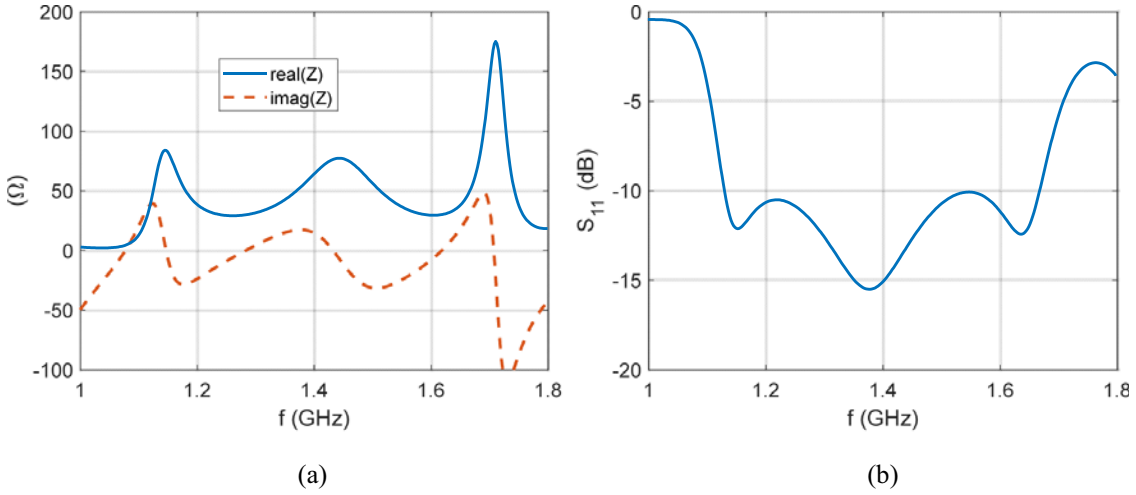

Figure 2. Simulated Z_{11} (a) (real part in continuous line and imaginary part in dashed line) and S_{11} (b) of the reference antenna.

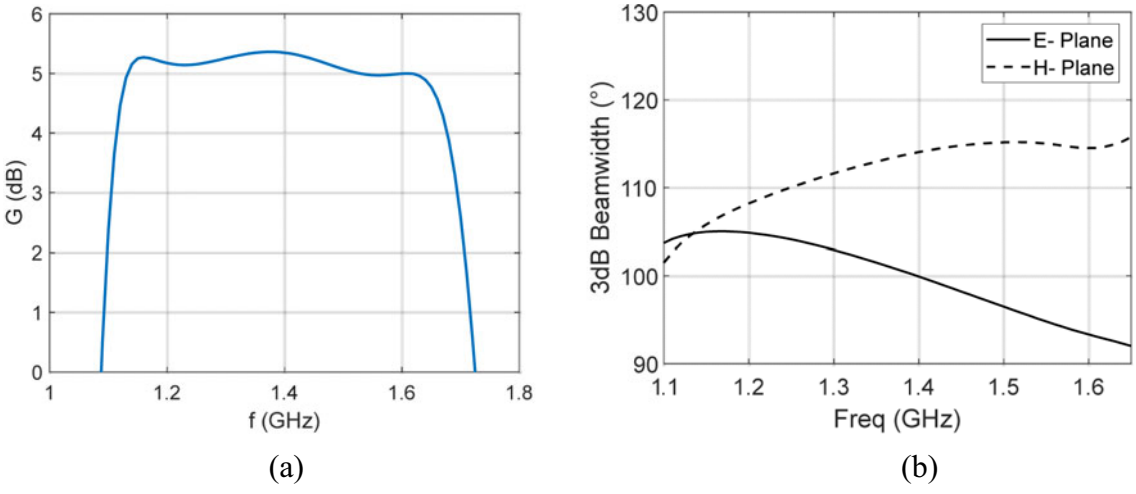

Figure 3. Broadside realized gain (a) and 3-dB beamwidth in E- and H-planes (b).

https://doi.org/10.1017/S1759078723001265 Published online by Cambridge University Press

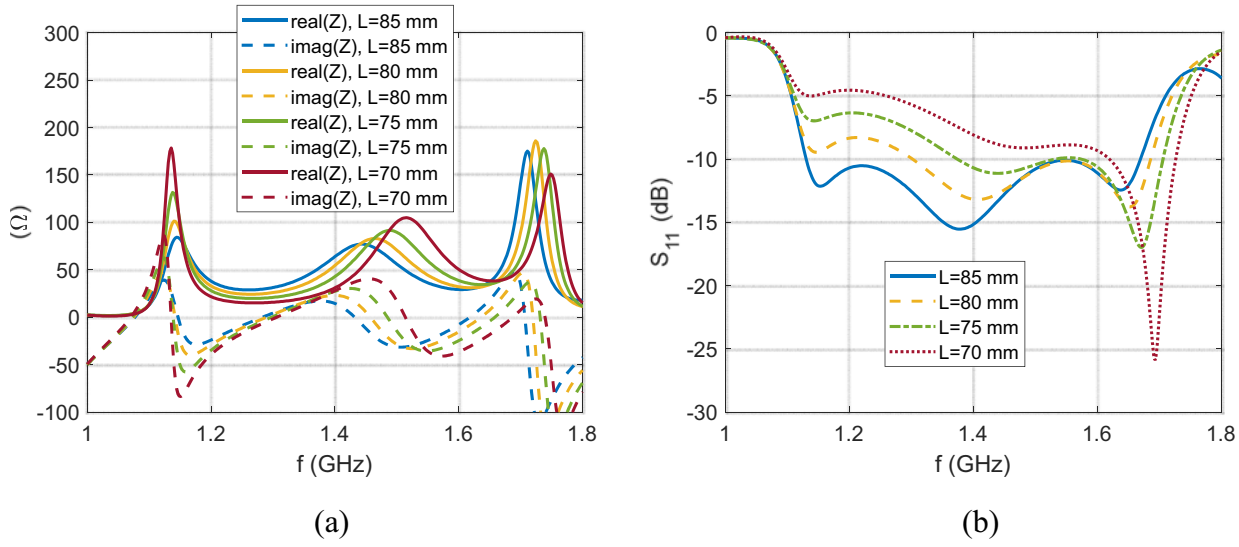

Figure 4. Simulated (a) input impedance (real part in continuous line and imaginary part in dashed line) and (b) reflection coefficient for various width L ($H_H = 35$ mm).

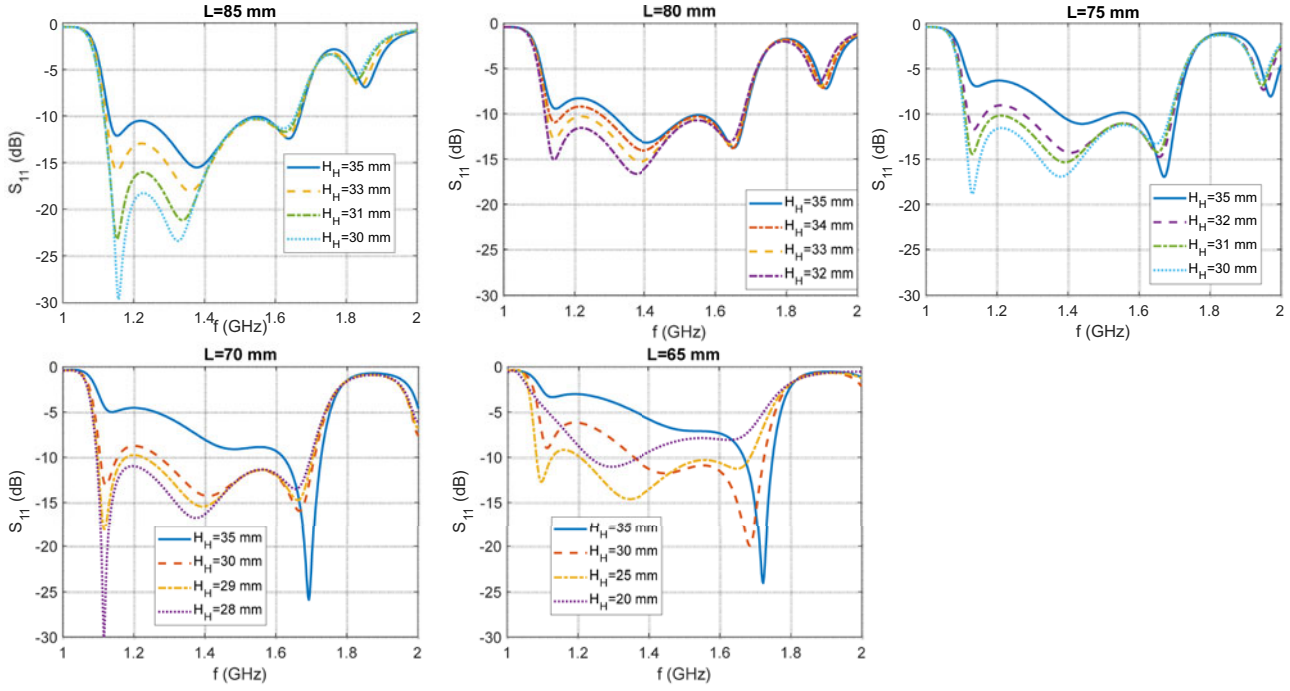

Figure 5. Simulated reflection coefficients for various H_H and L between 85 and 65 mm.

(H_H) is the most beneficial for impedance bandwidth enlargement of the antenna considering a relatively small cavity width.

Considering the antenna described in section "Planar antenna," the cavity width L is varied from 85 to 70 mm in a first time; the other parameters are identical to the ones in Table 1 (optimized for $L = 85$ mm). The simulated impedance and reflection coefficient are given in Fig. 4. When this width is reduced, the magnitudes of the first and second resonances increase, unmatching the structure for the lowest frequencies and reducing the bandwdith (BW). This is due to the coupling between the ME dipole and the cavity walls parallel to the exciting probe. In fact, when the width L is reduced, these walls are closer to the elements and the coupling increases. We also note a frequency shift of the second resonance (magnetic dipole), as well as, more slightly, of the third resonance.

In a second time, starting from the cavity wall height $H_H = 35$ mm, this parameter is reduced for various cavity width L between 85 and 60 mm. The simulated reflection coefficients are represented in Fig. 5. For $L = 85$ mm, reducing H_H of a few millimeters improves the matching and the BW is similar; in this case, there is no benefit in reducing H_H. For $L = 80$ and 75 mm, the antenna with $H_H = 35$ mm is not matched, whereas it becomes matched for a lower value of H_H (33 mm for $L = 80$ and 31 mm for $L = 75$ mm). For $L = 70$ mm, a wide BW is achieved for $H_H = 28$ mm; finally, for $L = 65$ mm, even by reducing H_H, a wide

https://doi.org/10.1017/S1759078723001265 Published online by Cambridge University Press

Table 2. BW of the planar antenna after optimization of the cavity height H_H for various cavity width L (reference central frequency of 1.38 GHz)

L (mm)	H_H (mm)	Impedance BW $\lvert S_{11}\rvert < -10$ dB (GHz)
85	35	1.13–1.67 (39.0%)
80	33	1.12–1.68 (40.4%)
75	31	1.11–1.69 (42.0%)
70	29	1.10–1.70 (43.5%)
65	25	1.2–1.69 (34.9 %)

BW could not be achieved. The results are summarized in Table 2. By reducing the cavity height H_H, the coupling between the walls and the ME dipole is minimized, and finally, an optimal value of H_H could be found for each L value, corresponding to a wide BW. Furthermore, it could be observed from Table 2 that an even wider BW could be achieved with a weaker value of L (down to 70 mm). This phenomenon will be advantageously used in the section Conformal case for conformal antennas.

Conformal case

The cylindrical conformation of the antenna is close to the cavity wall height modification proposed previously. In fact, this conformation is made in the direction orthogonal to the electric dipole (corresponding to the Y axis) as this configuration is the most beneficial for the wideband behavior of the antenna [20]. A schematic of the conformation can be seen in Fig. 6. The cavity walls in E-plane become rounded on top, whereas the cavity walls in H-plane become smaller than those in the planar case. The cavity-backed antenna can be integrated into a cylindrical or partially cylindrical carrier made from conductor material, non-conductor material, or both.

The electric dipole is conformed to a cylinder of radius R, and the cavity walls follow the cylinder shape. H_E is fixed to $\lambda_g/4$ with respect to the ME magnetic dipole resonance constraint. H_H can vary within the range $[0,H_E]$ depending on the radius R.

In this configuration, the length H_H and the width L are directly linked to the conformation radius R according to the following formulas:

$$H_H = H_E - R.\left(1 - \cos\left(\sin^{-1}\left(\frac{L}{2R}\right)\right)\right) \quad (1)$$

$$L = 2 \times \sqrt{R^2 - (R - H_E + H_H)^2} \quad (2)$$

These two equations impose that for a given radius R, a unique value of H_H corresponds to one value of L; in the optimization step (below), only L is tuned, as H_H depends on this parameter. The criteria is to cover the whole GNSS band, but not more, and ideally with an antenna as small as possible. In other terms, if for a given conformation radius R and a given width L, the achieved bandwidth is larger than the GNSS band from 1.16 to 1.61 GHz, then the width L can be optimized to a value corresponding to a bandwidth covering only the GNSS band (the value of H_H being affected by the variation of L).

The variation of L impacts both the height H_H and the distance between the ME dipole and the cavity. Figure 7 shows, for a chosen value of $R = 44$ mm, the evolution of the behavior of the antenna input impedance for different values of L.

We can observe a very similar behavior compared to the planar case, except that the effects of size reduction are stronger. When L is large and H_H is smaller than 20 mm, the electric dipole resonance is shifted out of the band of interest as it behaves like a free space ME dipole (no coupling between cavity and radiating element).

In Table 3 are summarized some values of external dimensions for optimized conformal antennas ; these results are found through numerical simulations. The criteria were impedance bandwidth and working frequencies for fixed cylindrical conformation radii. During the optimization process, the width L was varied in a first time, and other parameters were optimized in a second time to reach a good impedance matching on the GNSS frequency band (mainly the lengths c and L_{dip}). All the presented results are with $H_E = 35$ mm for the reasons exposed previously. We note that L_{min} is the smallest width L, allowing to cover all GNSS bands with a wideband behavior (for a given conformation radius R).

We can see that the values L_{min} and H_H decrease when the radius of conformation R decreases. In fact, the coupling between the radiating element and the cavity becomes weaker if the conformation radius R is decreased, which can be compensated by reducing the cavity width L (because the height H_H is higher for a smaller width, and the cavity wall then comes closer to the radiating element). Although other parameters are optimized for each conformation radius R, the optimization of the width L is the key parameter in this process. The results presented in Table 3 lead to conclude that decreasing the radius of conformation brings miniaturization of the antenna without significantly impacting the impedance behavior of the antenna. It has to be noted that without compensating for the coupling reduction due to the conformation by optimizing the cavity width, wideband behavior cannot be achieved. As can be seen from Table 3, the 3-dB beamwidth is affected mainly in the H-plane with a wider beamwidth, which is an advantage for the targeted application. It is to be noted that

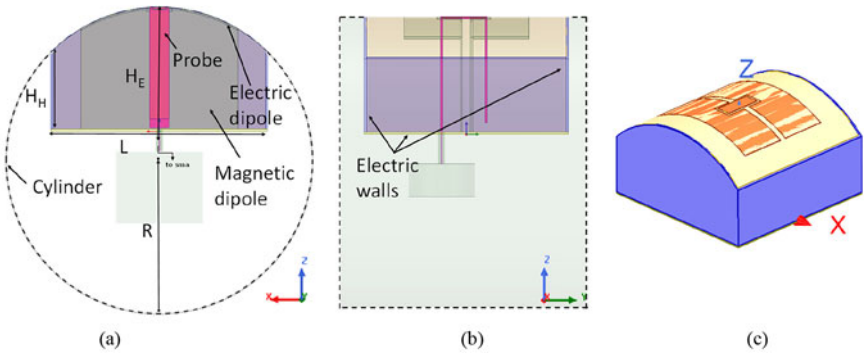

Figure 6. Cut-views of antenna conformation in (a) H-plane and (b) E-plane; (c) 3D view.

https://doi.org/10.1017/S1759078723001265 Published online by Cambridge University Press

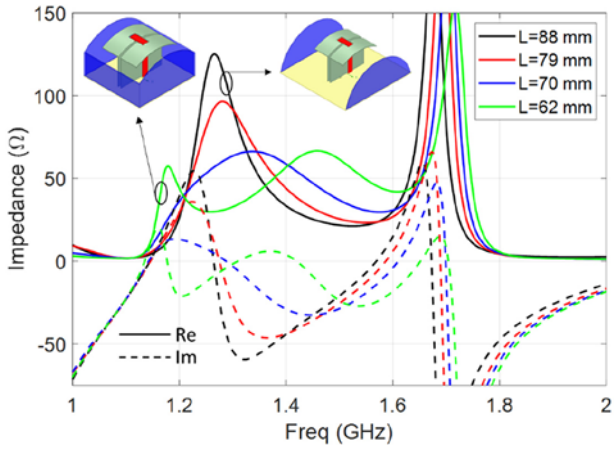

Figure 7. Variation of input impedance versus L for $R = 44$ mm and $H_E = 35$ mm (real part in continuous line and imaginary part in dashed line).

Table 3. Dimensions of the optimized conformal antennas for different values of conformation radius

R (mm)	L_{min} (mm)	H_H (mm)	Impedance BW $\lvert S_{11}\rvert < -10$ dB (GHz)	E-plane 3 dB beamwidth at 1.16 and 1.61 GHz	H-plane 3 dB beamwidth at 1.16 and 1.61 GHz
∞	85	35	1.13–1.67 (39.0%)	105°/92°	105°/115°
100	75	28	1.16–1.63 (33.7%)	107°/101°	105°/116°
77.5	70	27	1.14–1.69 (38.8%)	108°/103°	106°/114°
50	64	24	1.16–1.63 (33.7%)	110°/111°	110°/115°
44	62	22.8	1.16–1.69 (37.2%)	110°/113°	111°/115°
40	60	22	1.16–1.64 (34.3%)	111°/118°	113°/116°

in comparison to the planar case, the enlargement of the 3 dB beamwidth in E- and H-planes is obtained with an antenna size decrease and a decrease of the cavity walls in H-plane H_H. A ground plane area reduction of 53.3% is obtained for a 40-mm radius cylindrical conformation compared to the reference planar antenna. This size reduction is only imputed to the conformation as the dielectric material inside the cavity remains the same. It is to be noted that in comparison to the planar case of discussed in section "Planar antenna" (results given in Fig. 3), the 3 dB beamwidth is more symmetric in E- and H-planes, especially within the small radius R.

Optimized antenna and measurement results

Based on the previous analysis of the impact of conformation on antenna behavior, an optimized ME antenna conformed to a 44-mm radius cylinder is proposed. The prototype of this antenna is shown in Fig. 8, surrounded by a holding frame fabricated using classical 3D printing material Acrylonitrile Butadiene Styrene (ABS) material with 60% material filling. The optimized dimensions shown in Table 3 take into account the small influence of the holding frame. This holding frame has the function to keep the

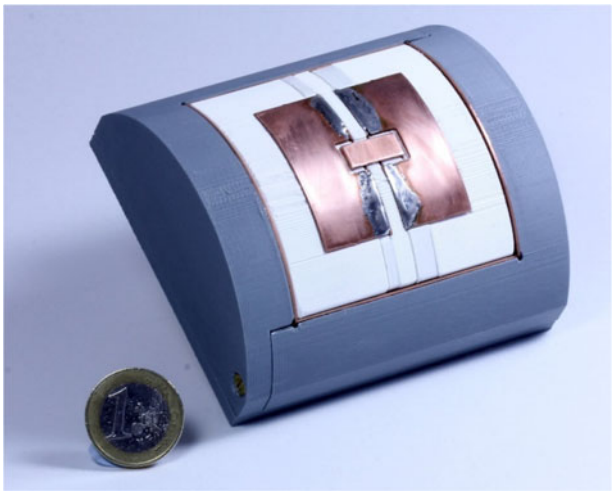

Figure 8. Prototype of the optimized conformal ME antenna ($R = 44$ mm).

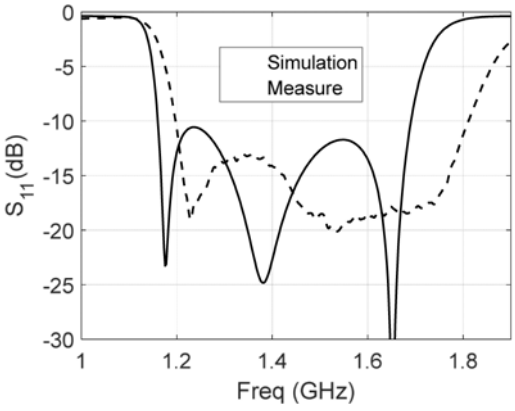

Figure 9. Simulated and measured $|S_{11}|$ of the conformal optimized antenna.

metallic cavity surrounding the antenna closed, as it would be if integrated into a carrier. It is used only for the characterization of the antenna. The integration of this antenna on a metallic carrier would require a slight modification of the proposed dimensions and thus is not shown here as the presented prototype validates the principle.

This structure exhibits external dimensions of $62 \times 62 \times 35$ mm^3. The substrate was fabricated with Preperm ABS300 material ($\varepsilon_r = 3$, $\tan\delta = 4.6 \times 10^{-3}$) using Ultimaker S5 3-D printer. It was measured using Agilent E8363C network analyzer for S parameters and MVG SG24 anechoic chamber for radiation properties. Measured and simulated S_{11} are visible in Fig. 9. We can note a good agreement with a small shift of 30 MHz (2,2%) between simulated and measured S_{11}, with 1.16–1.69 GHz for the simulation and 1.20–1.81 GHz (40,5%) for the prototype. The difference is mainly due to the fabrication process and its uncertainties; this shift is attributed to the gaps between the substrate pieces, which is required for the assembly; the repartition of these gaps is not homogeneous, depending on how the manufactured elements (by 3D printing technology) interlock. However, the measurement validates the principle and the considered substrate's electromagnetic properties.

Measured and simulated realized broadside gain and simulated 3 dB beamwidth in E- and H-planes versus frequency are

https://doi.org/10.1017/S1759078723001265 Published online by Cambridge University Press

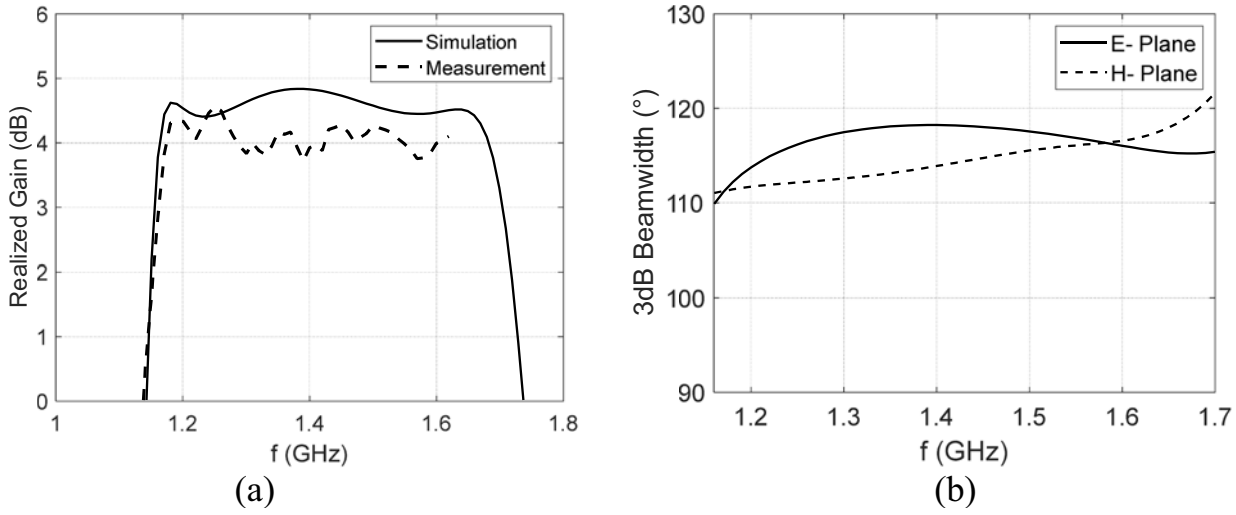

Figure 10. Simulated and measured realized gain (a) and simulated 3 dB beamwidth (b) of the conformal antenna.

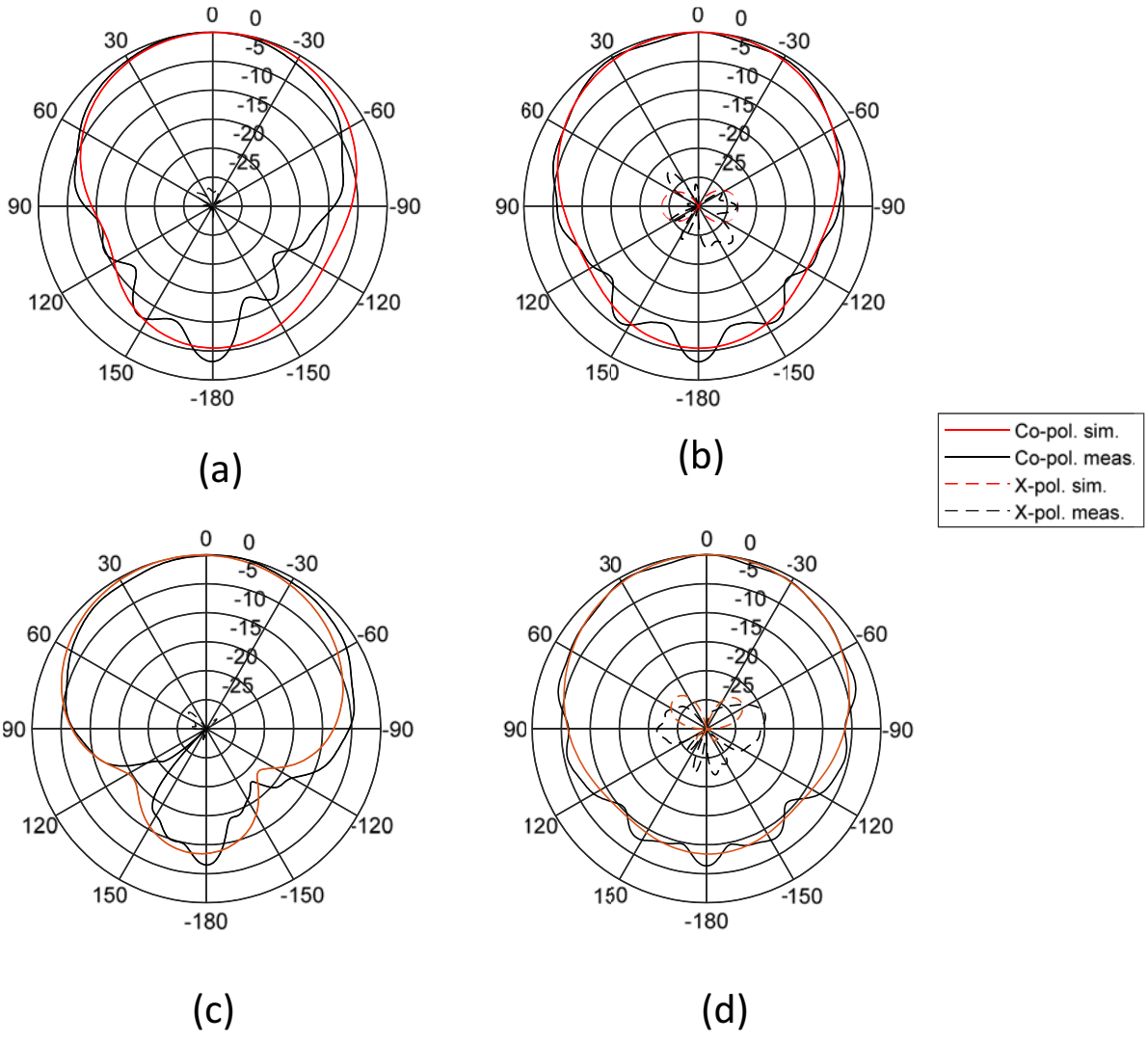

Figure 11. Simulated and measured normalized radiation pattern in E- and H-planes (a and b) at 1.20 GHz and (c and d) at 1.61 GHz.

https://doi.org/10.1017/S1759078723001265 Published online by Cambridge University Press

shown in Fig. 10. Measured 3 dB beamwidth is 106° and 113° for E- and H-planes, respectively, at 1.2 GHz and 116° and 122° for E- and H-planes at 1.61 GHz, corresponding to a maximum of 6° compared to simulation.

Measured gain has a maximum difference of 1.1 dBi with simulation in the 1.2–1.61 GHz frequency band and a mean gain value of 4.2 dBi.

These gain values and the radiation patterns observed in Fig. 11 show smaller front to back ratio when compared to classical ME antennas. This is explained by the small dimensions of the ground plane compared to the wavelength ($0.285 \times 0.285\lambda_0^2$) [23, 24], but a good agreement is obtained with simulations. Out of the working bandwidth, the gain drops drastically, which can be an advantage for sensitive applications such as GNSS applications. Radiation efficiency is around 90% between 1.2 and 1.61 GHz. The measured gain variations are attributed to the measurement system uncertainties, which are given by the supplier up to 1 dB. The achieved 3 dB beamwidth values are closer in E- and H-planes for conformal case than for planar antenna of section 2; this can be explained because the configuration is closer to a free space ME antenna. We also note a good symmetry of the radiation pattern, which is typical of ME antennas.

Conclusion

In this article, a study of the impact of the cylindrical conformation of linear polarisation (LP) cavity-backed ME antenna with a feeding probe located outside of the magnetic dipole was proposed. This study shows the key role of the coupling between the radiating element and the cavity in the wideband response of such structure; as the conformation radius becomes small, the cavity wall height decreases and the coupling is attenuated, and this phenomenon can be compensated by reducing the cavity size. In this case, the wall will be closer to the radiating element without being at the same level. Moreover, wideband behavior is maintained. The level of miniaturization directly depends on the conformation radius considered and increases when the radius decreases. An optimized version of conformal antenna ($R = 44$ mm) was fabricated to be integrated into a cylindrical carrier using low-cost additive manufacturing. A footprint area reduction of 46% was observed compared to the planar optimized antenna using the same substrate to fill the cavity. The antenna exhibits 37.2% bandwidth, covering all GNSS bands, and a stable gain with a mean value of 4.5 dBi.

Funding statement. This work was funded by the French-German Research Institute of Saint-Louis (ISL), France.

Competing interests. The authors report no conflict of interest.

References

1. **Yinusa KA** (2018) A dual-band conformal antenna for GNSS applications in small cylindrical structures. *IEEE Antennas and Wireless Propagation Letters* **17**(6), 1056–1059.
2. **Zhong Z-P, Zhang X, Liang JJ, Han CZ, Fan ML, Huang GL, Xu W and Yuan T** (2019) A compact dual-band circularly polarized antenna with wide axial-ratio beamwidth for vehicle GPS satellite navigation application. *IEEE Transactions on Vehicular Technology* **68**(9), 8683–8692.
3. **Johannsen U, Schulpen R, Manders LCW and Engel R** (2021) GNSS antenna design for underwater mine-disposal-vehicles. In *2021 15th European Conference on Antennas and Propagation (EuCAP)*, Dusseldorf, Germany, March, 1–5.
4. **Tinoco-S. AF, Ribeiro-Filho PC, Heckler MVT, Lacava JCDS and Pereira-Filho OMC** (2016) Fast predesigning of circumferential arrays of probe-fed microstrip antennas. In *2016 10th European Conference on Antennas and Propagation (EuCAP)*, Davos, 1–4.
5. **Luk KM and Wong H** (2006) A new wideband unidirectional antenna element. *International Journal of Microwave and Optical Technology* **1**(1), 10.
6. **Ge L and Luk KM** (2013) A magneto-electric dipole antenna with low-profile and simple structure. *IEEE Antennas and Wireless Propagation Letters* **12**, 140–142.
7. **Ding C and Luk K-M** (2016) Low-profile magneto-electric dipole antenna. *IEEE Antennas and Wireless Propagation Letters* **15**, 1642–1644.
8. **Luk KM and Wu B** (2012) The magnetoelectric dipole – A wideband antenna for base stations in mobile communications. *Proceedings of the IEEE* **100**(7), 2297–2307.
9. **Li M, Luk K-M, Ge L and Zhang K** (2016) Miniaturization of magneto-electric dipole antenna by using metamaterial loading. *IEEE Transactions on Antennas and Propagation* **64**(11), 4914–4918.
10. **Zhang X, Jiao Y, Weng Z, Zhang Y and Feng S** (2019) Wideband magneto-electric dipole antenna with a claw shaped reflector for 5G communication systems. *Microwave and Optical Technology Letters* **61**(9), 2098–2104.
11. **Tao J, Feng Q and Liu T** (2018) Dual-wideband magnetoelectric dipole antenna with director loaded. *IEEE Antennas and Wireless Propagation Letters* **17**(10), 1885–1889.
12. **Neetu GPP, Tiwari VN and Marwah SS** (2016) A novel ultra-wide band magneto-electric dipole antenna with a cavity reflector. *Progress in Electromagnetics Research C* **63**, 143–152.
13. **An WX, Lau KL, Li SF and Xue Q** (2010) Wideband E-shaped dipole antenna with staircase-shaped feeding strip. *Electronics Letters* **46**(24), 1583.
14. **Causse A, Bernard L, Sharaiha A and Collardey S** (2021) Low profile multiband magnetoelectric antenna for GNSS and telemetry. In *2021 IEEE Conference on Antenna Measurements & Applications (CAMA)*, France.
15. **Chang L, Zhang J-Q, Chen -L-L and Li B-M** (2018) Bandwidth-enhanced cavity-backed magneto-electric dipole antenna. *IEEE Access* **6**, 62482–62489.
16. **Feng B, Chung KL, Lai J and Zeng Q** (2019) A conformal magneto-electric dipole antenna with wide H-plane and band-notch radiation characteristics for Sub-6-GHz 5G base-station. *IEEE Access* **7**, 17469–17479.
17. **Causse A, Rodriguez K, Bernard L, Sharaiha A and Collardey S** (2021) Compact bandwidth enhanced cavity-backed magneto-electric dipole antenna with outer Γ-Shaped probe for GNSS bands. *Sensors* **21**(11), 3599.
18. **Chen C and Zheng H** (2017) Design of a dual-band conformai antenna on a cone surface for missle-borne. In *2017 Sixth Asia-Pacific Conference on Antennas and Propagation (APCAP)*, Xi'an, October, 1–3.
19. **Sahoo R and Vakula D** (2017) A cylindrical conformal antenna for GPS application. In *2017 8th International Conference on Computing, Communication and Networking Technologies (ICCCNT)*, Delhi, July, 1–4.
20. **Kellomäki T** (2012) Analysis of circular polarization of cylindrically bent microstrip antennas. *International Journal of Antennas and Propagation* **2012**, 1–8.
21. **Causse A, Bernard L, Collardey S and Sharaiha A** (2022) Small conformal cavity-backed magnetoelectric antenna for GNSS bands. In *16th European Conference on Antennas and Propagation (EuCAP)*, March, Madrid, Spain.
22. Ansys HFSS 3D High frequency simulation software. https://www.ansys.com/fr-fr/products/electronics/ansys-hfss (accessed 19 May 2022).
23. **Idayachandran G and Nakkeeran R** (2016) Compact magneto-electric dipole antenna for LTE femtocell base stations. *Electronics Letters* **52**(8), 574–576.
24. **Liu Y, Li M, Zhang Y, Wu Y and Xia X** (2017) Compact magneto-electric dipole antenna with low-profile for LTE femtocell base stations. In *2017 Sixth Asia-Pacific Conference on Antennas and Propagation (APCAP)*, Xi'an, October, 1–3.

https://doi.org/10.1017/S1759078723001265 Published online by Cambridge University Press

Alexandre Causse received the engineer degree in electronics from the Ecole Supérieure d'Ingénieurs en Electronique et Electrotechnique (ESIEE), Paris, France, and M.S. in RF communication systems from Gustave Eiffel University, Paris, France, both in 2019. In 2022, he achieved a PhD in antenna design focusing on small cavity-backed wideband antennas for GNSS applications with the French-German Research Institute of Saint-Louis (ISL), Saint-Louis, France, and the Institut d'Electronique et des Technologies du numeRique (IETR), University of Rennes, France. He then joined the Direction Générale de l'Armement (DGA), Rennes, France, as an RF engineer focusing on electronic warfare systems.

Loïc Bernard graduated in Electronics and Communication Systems from the National Institute of Applied Sciences (INSA) of Rennes, France, in 2000. After this engineer degree, he received the PhD degree in electrical engineering from INSA of Rennes, France, in 2003. Then, he joined the French-German Research Institute of Saint-Louis (ISL), France, in May 2004 as a research scientist. He received the "Habilitation à Diriger des Recherches" degree from the University of Rennes 1, Rennes, France, in 2017. In 2021, he also became an associate member of the Institute of Electronic Telecommunication of Rennes (IETR). He is involved in the electronics instrumentation of flying systems with very high dynamics for aerodynamic and ballistic research; his research interests include antennas, antenna arrays, microwave circuits, and metamaterials.

Sylvain Collardey received his PhD degree in telecommunication from the University of Rennes 1, France, in 2002. He graduated in Electronics and Telecommunication Engineering from the University of Rennes 1 in 1998. Currently, he is an associate professor at the University of Rennes and is involved as a researcher in the Department of Antenna and Microwave Devices, IETR. His research interests include characterization and development of small antennas, superdirective antennas, numerical modeling, periodic and non-periodic structures (EBG, metasurfaces, etc.), and RFID technology. He has published more than 100 revue papers and conference communications.

Ala Sharaiha received the PhD and Habilitation à Diriger la Recherche (HDR) degrees in telecommunication from the University of Rennes 1, France, in 1990 and 2001, respectively. Currently, he is a full professor at the University of Rennes 1 and the Co-Head of the Antennas and Microwave Devices Department at the IETR research laboratory (Institute of Electronics and Telecommunications in Rennes). He has graduated/mentored more than 42 PhD students/postdocs and co-authored with them. He has authored or co-authored more than 500 journal and conference papers, concerning antenna theory, analysis, designs, and measurements. He holds 14 patents. His published works have been cited over 2500 times in Google Scholar. His current research interests include small antennas, broadband and UWB antennas, reconfigurable antennas, printed spiral and helical antennas, and antennas for mobile communications. He is presently a French delegate member of the European Association on Antennas and Propagation (EuRAAP) and a member of the small antennas working group of EuRAAP. He is a senior member of the IEEE and is a reviewer for the IEEE APS, IEEE AWPL, the IET Letters, and the IET Microwave Antennas Propagation. He was the conference Chairman of the 11th International Canadian Conference Antenna Technology and Applied Electro-Magnetics (ANTEM), held at Saint-Malo in France, 2005.

https://doi.org/10.1017/S1759078723001265 Published online by Cambridge University Press